High-Performance Missile Synthesis with Trajectory and Propulsion System Optimization

P. K. A. Menon,* V. H. L. Cheng,† C. A. Lin,* and M. M. Briggs‡
Integrated Systems Inc., Palo Alto, California

Synthesis of a high-performance two-pulse-motor-propelled missile by simultaneous optimization of trajectory and propulsion systems in two operational scenarios is described. This work employed a quasiNewton parameter optimization scheme with penalty functions to meet terminal and path constraints. The trajectory control variables were parameterized using piecewise linear open-loop commands and piecewise constant linear feedback gains. The pulse motor parameters optimized were pulse split, average thrust levels, neutrality factors, pulse burn times, and the interpulse delay. Optimization of the rocket motor thrust time curve in addition to the trajectory increased the range by up to 11% when compared with the trajectories optimized with originally specified rocket motor propulsion data.

Introduction

THE pulse motor propulsion concept has demonstrated significant performance payoffs for medium range air-to-air missiles.[1,2] For this class of missiles, the pulse motor propulsion scheme has led to significant improvements in the outer launch boundary and the F-pole. The present research examines the use of pulse motor propulsion for air-to-surface missiles. Specifically, the objective of the study is to generate optimal trajectory and pulse motor designs in two operational scenarios: 1) Low-altitude constrained mission with a minimum specified terminal speed; 2) High-altitude mission with a specified minimum dynamic pressure and a minimum average terminal speed. The "average terminal speed" in the present context is defined as the average missile speed while traversing through a hemispherical annular region specified about the target.

The trajectory control variables are angle of attack and angle of sideslip while the motor parameters to be optimized consist of pulse split, neutrality factors (normalized slope of the pulse thrust time curve), burn times, and interpulse delay time. The total propellent weight and the all-up weight are assumed to be fixed. The penalties in selecting too high or too low thrust levels with long burn durations are included through appropriate specific impulse degradation. Though the present thrust modeling is somewhat simplistic, it is adequate for generating a first-cut estimate of the propulsion system parameters.

Ideally, an automatic missile synthesis scheme should handle aerodynamic shape optimization also, perhaps along the lines of Ref. 3. However, numerical fluid dynamic computations are currently far from routine and can often be very expensive. In view of this fact, the current research effort will deal only with propulsion system and trajectory optimization. A quasi-Newton parameter optimization algorithm is employed in the present work with penalty functions to meet terminal and path constraints. The trajectory control variable parameterization using piecewise linear open-loop commands and piecewise constant linear feedback gains will also be discussed.

Received Sept. 3, 1985; revision received April 2, 1986. Copyright © 1985 by Integrated Systems, Inc. Published by the American Institute of Aeronautics and Astronautics, Inc., with permission.

*Research Scientist. Member AIAA.
†Senior Research Scientist. Member AIAA.
‡Manager, Missile Systems Division. Associate Fellow AIAA.

Missile Modeling

A point-mass model for missile flight over flat, nonrotating earth is used to represent the missile trajectory dynamics in the present work. This model is given by the six following nonlinear ordinary differential equations as:

$$\dot{V} = \frac{F_1}{m} - g\sin\gamma \tag{1}$$

$$\dot{\gamma} = \frac{g}{V}\left(\frac{F_3}{mg} - \cos\gamma\right) \tag{2}$$

$$\dot{\chi} = -F_2/(mV\cos\gamma) \tag{3}$$

$$\dot{x} = V\cos\gamma\cos\chi \tag{4}$$

$$\dot{y} = V\cos\gamma\sin\chi \tag{5}$$

$$\dot{h} = V\sin\gamma \tag{6}$$

with

$$\begin{bmatrix} F_1 \\ F_2 \\ F_3 \end{bmatrix} = \begin{bmatrix} \cos\alpha\cos\beta & \sin\beta & -\sin\alpha\cos\beta \\ -\cos\alpha\sin\beta & \cos\beta & \sin\alpha\sin\beta \\ \sin\alpha & 0 & \cos\alpha \end{bmatrix} \begin{bmatrix} F_A \\ F_S \\ F_N \end{bmatrix} \tag{7}$$

where

$$F_A = -qsC_A + T$$

$$F_S = -F_4\sin\beta$$

$$F_N = F_4\cos\beta\sin\alpha$$

$$F_4 = qsC_N/\sqrt{\sin^2\beta + \cos^2\beta\sin^2\alpha}$$

$$\alpha_T = \cos^{-1}(\cos\alpha\cos\beta)$$

In these expressions, V is the total missile speed, γ the flight path angle, χ heading angle, x the down range, y cross range, h altitude, and α,β are the angle of attack and the angle of sideslip, the trajectory control variables in the present problem. The axial force coefficient C_A is a function of Mach number M, while the normal force coefficient C_N is a function of M and the total angle of attack α_T. The thrust T and mass m are functions of the average pulse thrust $\bar{T}_1, \bar{T}_2$, the neutrality factors η_1, η_2, the pulse burn durations τ_{p1}, τ_{p2}, the interpulse delay time τ_c and the impulse split μ. A typical thrust

and mass profile is given in Fig. 1. The variables q and s are the dynamic pressure and the reference area, respectively.

The pulse motor thrust and mass histories are modeled using piecewise continuous functions of time, with the assumption that the specific impulse is constant throughout each pulse. During trajectory runs, the expended inert mass during a pulse is absorbed into the propellant mass, leading to a slightly lower specific impulse. The thrust and mass profiles for a pulse beginning at time t_0 with burn time τ_p are defined by the following formula for $t \in [t_0, t_0 + \tau_p]$:

$$T(t) = \bar{T}\left\{1 - \eta + 2\eta\frac{(t - t_0)}{\tau_p}\right\} \tag{8}$$

$$m(t) = m(t_0) - \frac{\bar{T}}{I_{sp}}\left[(1-n)(t-t_0) + \frac{\eta}{\tau_p}(t-t_0)^2\right] \tag{9}$$

Here, $(t - t_0)$ is the elapsed time since pulse ignition and I_{sp} is the specific impulse. The average specific impulse for the higher-thrust pulse was fixed. The specific impulse for the lower-thrust pulse is then computed using an empirical relation. Thus, suppose the first pulse has higher thrust with specific impulse I_{sp_1}. The average specific impulse of the second pulse is empirically defined as

$$I_{sp_2} = I_{sp_1}(R_T)^{\kappa} \tag{10}$$

where $R_T = \bar{T}_2/\bar{T}_1$, the ratio of average thrust levels. The exponent κ on the right-hand side of Eq. (10) is determined from experimental data for this class of pulse motors. Since the value of I_{sp_1} affects the value of R_T, Eq. (10) is not explicit. Hence, a one step recursion is set up to compute both values. This equation penalizes the selection of too high or too low average pulse thrust values by the optimization algorithm. Moreover, since the total propellant weight is fixed, this would indirectly constrain the pulse burn durations also. The thrust neutrality factor is next defined as

$$\eta = 1 - T_0/\bar{T} = T_b/\bar{T} - 1 \tag{11}$$

where T_0 is the initial thrust of a pulse and T_b is the final thrust of a pulse. The neutrality factor is constrained as

$$-1 \le \eta \le 1 \tag{12}$$

Equations (1–12) are next implemented in a computer simulation. Several simulation runs were made with a fourth-order Runge-Kutta numerical integration scheme with linearly interpolated atmospheric and aerodynamic data to ensure correctness of the implementation and to get a feel for the effect of optimization parameters.

Trajectory and Propulsion System Optimization

The combined trajectory and propulsion system optimization problem may be stated as: Given the differential constraints (1-7), Eqs. (8-11) and the simple bounds (12), select the pulse motor parameters and the trajectory control variable histories $\alpha(t)$ and $\beta(t)$ to maximize the final downrange $x(t_f)$ at the free final time t_f. Depending on the selected mission scenario, additional constraints are imposed on this optimization problem as follows:

1) Low-altitude mission
Maximum altitude constraint:

$$h(t) \le h_{max} \tag{13}$$

Final speed:

$$V(t_f) \ge V_f \tag{14}$$

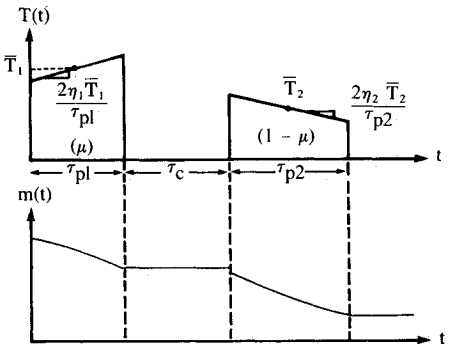

Fig. 1 Thrust and mass profiles.

2) High-altitude mission
Minimum dynamic pressure constraint:

$$q(t) \ge q_{min} \tag{15}$$

Specified average terminal speed:

$$V_{av} \ge V_A \tag{16}$$

where

$$V_{av} = \frac{R_1 - R_2}{t_2 - t_1} \tag{17}$$

In expression (17), R_1 and R_2 define the radii of a hypothetical hemispherical annular zone specified about the target. The radius at time t is computed as

$$R(t) = \sqrt{h^2(t) + y^2(t) + \left[x(t_f) - x(t)\right]^2} \tag{18}$$

with $R(t_1) = R_1$, $R(t_2) = R_2$. In both of these mission scenarios, the final altitude and the final crossrange are required to be zero. Furthermore, the trajectory control variables, the angle of attack and the angle of sideslip are bounded. Thus,

$$h(t_f) = 0, \quad y(t_f) = 0 \tag{19}$$

$$|\alpha| \le \alpha_{max}, \quad |\beta| \le \beta_{max} \tag{20}$$

Since the missile sometimes operates close to the terrain in the low-altitude mission, trajectories with negative altitude can emerge from the optimization process. These are clearly not admissible from a practical point of view. Hence, in order to eliminate such cases, a terrain limit is next imposed:

$$h(t) \ge 0 \tag{21}$$

The task remaining after modeling and constraint definition is the choice of the optimization technique. Note that the defined problem is a combined parameter and trajectory optimization problem.

The numerical computation techniques for optimal atmospheric trajectories continues to be an active research area as evidenced by the recent literature.[4-12] The approaches employed appear to belong to two distinct categories: the ones that are based on the solution of the two-point boundary value problem arising from the application of Pontriagin's minimum principle,[4,5,13] and the ones that use mathematical programming[6-11] by parameterizing the state control histories. The latter appears to have been more popular in the applications work, possibly because of their relative robustness. In

the present work, the combined parameter and trajectory optimization problem will be handled using a quasi-Newton[14] for minimization in conjunction with penalty functions for satisfying path and terminal constraints.

In order to convert the trajectory optimization problem into a mathematical programming problem, the control variables and possibly the state variables need to be parameterized over time. Several schemes have been reported for this purpose: polynomials,[15] cubic splines,[7-9] and Chebychev polynomials,[6] Rayleigh-Ritz type parameterizations[11] being typical. If the control variables alone are parameterized, one requires a numerical simulation of the missile system to generate state variable histories, constraint violations, and performance index. On the other hand, if the state variables are also parameterized as in Refs. 6 and 7, the optimization problem becomes completely algebraic. Note that the parameterized trajectory optimization results are suboptimal and the near-optimality of the solution is entirely controlled by the fidelity of parameterization. Thus, in a given problem, one should parameterize as few trajectory variables as possible. In any case, the parameterization is an arbitrary device in that it is difficult to come up with a "best" scheme that will work in every problem. In most mathematical programming algorithms, the computation time is a strong function of the number of optimized parameters. Hence, it is only logical to select a parameterization scheme that can represent a large class of functions with as few parameters as possible. In an early work on trajectory optimization, Kelley and Denham[16] have pointed out that the use of cubic spline functions for parameterization may offer an attractive compromise between the number of parameters and the class of functions generated.

In the present problem, numerical experimentation with the missile simulation revealed that an open-loop parameterization of the trajectory control variables using cubic splines for the low-altitude mission required a large number of knots in order to prevent frequent violation of the maximum altitude constraint and the terrain limit. This difficulty arises largely because of the high kinetic energy of the missile during a pulse burn. A typical optimization run with spline parameterization demanded in excess of 20 hours of CPU time on a VAX 11/750 digital computer. Since this is clearly not acceptable, alternate parameterization schemes were sought.

The trajectory optimization problem is first cast as a closed-loop guidance problem wherein the control variables are made functions of the system states and open-loop commands. The simplest scheme in this class consists of piecewise linear open-loop commands and piecewise constant linear feedback gains, thus producing a combination of open-loop and closed-loop parameterization. The exact form of such a "guidance law" has to be determined for each problem, primarily through engineering judgment and numerical experimentation. It is to be noted, however, that no justification can be offered for this parameterization. It is an arbitrary device just like any other parameterization scheme. Depending on the mechanization, this scheme is capable of generating piecewise continuous functions in addition to the usual piecewise smooth functions or smooth functions generated by other types of parameterizations outlined earlier in this paper. In order to maintain uniformity, a similar scheme is employed for the high-altitude mission also.

For the low-altitude mission, the form of parameterization used is

$$\alpha = k_1(h_r - h) - k_2\dot{h} \tag{22}$$

$$\beta = k_3 V\cos\gamma(\chi_r - \chi) \tag{23}$$

Here, h_r and χ_r are piecewise linear functions of time. The gains k_1, k_2 and k_3 are piecewise constant functions of time. In an optimization run, these are the guidance parameters to be optimized. The term $V\cos\gamma$ appearing on the right-hand side of Eq. (23) is motivated from a desire to partially offset the coupling between the vertical and horizontal dynamics in the missile model. The altitude rate feedback in Eq. (22) provides a measure of damping in the vertical plane.

Using the observation that in the absence of the altitude constraint, a significant portion of a high-energy missile trajectory consists of a nearly parabolic path, an alternate parameterization scheme is employed for the high-altitude mission. Along a parabolic trajectory, the flight path angle is a linear function of time. Consequently, an open-loop flight path angle command history consisting of a central linear segment and two constant end segments is constructed, as shown in Fig. 2. Since the length of each segment is unknown, the temporal location of the transitions are also optimized. Thus, in Fig. 2, γ_1, γ_2, γ_3, t_1 and t_2 are selected by the optimization scheme. The possibility of a jump at t_2 is incorporated to handle rapid changes in the path angle that may be required while the missile is descending at a high velocity. Thus, the angle of attack for the high-altitude mission is parameterized as

$$\alpha = k_4\frac{V}{g}(\gamma_r - \gamma) \tag{24}$$

The angle of side slip parameterization employed is the same as the low-altitude mission, Eq. (23). The term V/g multiplying the right-hand side of Eq. (24) partially compensates for its inverse appearing in the $\dot{\gamma}$ in Eq. (2). This ensures that at higher missile velocities, smaller flight path angle errors would generate larger angles of attack. The linear feedback gain parameter k_4 is a piecewise constant function of time.

Using this control variable parameterization, the state variable histories and the performance index can be computed from the missile simulation. In order to handle the path constraints, a procedure needs to be set up next. In a problem wherein the state variables are also parameterized, for example, as in Refs 6 and 7, the path constraints can be set up at each parameterization interval. On the other hand, with only control variable parameterization, the path constraints need to be propagated to the final time as integral squares of the violation accumulated over the whole trajectory. For an excellent account of this approach, the reader is directed to Ref. 10. No specific schemes are required for handling the terminal constraints. With the foregoing, the combined trajectory and parameter optimization problem is now in standard nonlinear programming form. Using penalty functions, this problem can be converted to an equivalent unconstrained parameter optimization problem.[10,13]

In the present work, a quasi-Newton[14] algorithm with finite-difference approximation for the gradients is used for parameter optimization. The method is iterative and hence requires an initial estimate of the parameters. A typical iteration starts at the current parameters ξ^i, with an estimate of the gradient vector G, a lower triangular matrix U and a

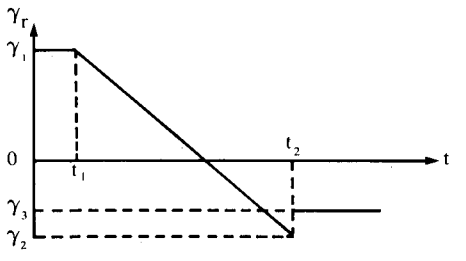

Fig. 2 Open-loop command parameterization for the high-altitude mission.

diagonal matrix E such that UEU^T is a positive-definite approximation to the current Hessian. The linear equations

$$UEU^T P = -G \tag{25}$$

are solved to generate the direction of search P. A scalar δ is next determined through a one-dimensional search in order to update the parameters as

$$\xi^{i+1} = \xi^i + \delta P \tag{26}$$

The value of δ is such that the updated parameter ξ^{i+1} provides a lower value of the performance index than ξ^i. The matrices U and E are then updated using the Davidon-Fletcher-Powell formula.[14]

A computer program is written to implement the missile simulation along with the quasiNewton minimization technique. Initial guess required to start the optimization procedure is generated by repeated missile simulation with a manual adjustment of input parameters. In a typical run, there are six motor parameters along with the open-loop command points and linear feedback gains to be selected. Four or five simulation runs were found adequate in the present case to generate the initial guess parameters for a given scenario.

Results and Discussions

Representative air-to-surface missile aerodynamic data were used to generate the results presented in this paper. The missile simulation scheme employed linear interpolation for aerodynamic coefficients with closely spaced data points and a fourth order Runge-Kutta scheme for numerical integration. A study was initiated during the first phase of the work to evaluate the effect of combined open-loop and closed-loop control variable parameterization on optimization results. To this end, two versions of optimization code were set up. The first version employed a completely open-loop spline parameterization for the control variables, while the second version used the combined open-loop and closed-loop parameterization. Optimization runs were made for both the high-altitude mission and the low-altitude mission. The results indicated that though the trajectories emerging from these studies exhibited some differences, the performance index was within 0.5% of each other. The convergence time, however, was different by a factor of 4, always in favor of the combined open-loop and closed-loop parameterization. It needs to be stressed here that this conclusion cannot claim uniform validity in all problems. Indeed, if the combined open-loop/closed-loop parameterization were inappropriate, it is possible that one would reach an opposite conclusion. However, the above exercise provided a measure of confidence in the control parameterization scheme used in the present work.

Though about 100 optimizations were carried out, only sample results would be presented here. For the low-altitude mission, the optimization results with a 1000 ft (304.8 m) altitude constraint will be discussed. The optimization process was started with an initial guess for the open-loop commanded altitude of 1000 ft (304.8 m) until the final time with a constant value for the linear feedback gain parameters k_1, k_2, k_3. The starting values of the gains were such that the missile flies at nearly constant altitude throughout with a vertical dive at the final time to meet final altitude and airspeed constraints. The initial guess values for the neutrality factors were zero, with equal division of burning time for the pulses, equal average thrust, and zero pulse delay time.

A converged trajectory for the low-altitude mission is shown in Figs. 3 and 4. The optimal angle of attack history is given in Fig. 5. This optimization required about 40 iterations consuming about 3 h on a VAX 11/750 machine. The optimized pulse motor thrust time curve given in Fig. 6 reflects the than half of the total propellant in the first pulse proved to be optimum and is consistent with the fact that the launch speed

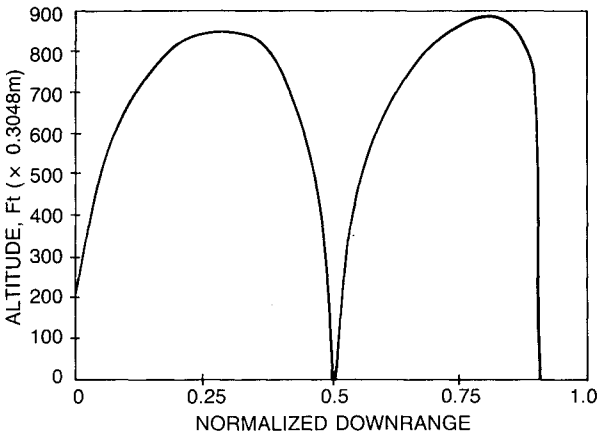

Fig. 3 Altitude constrained trajectory altitude vs normalized downrange.

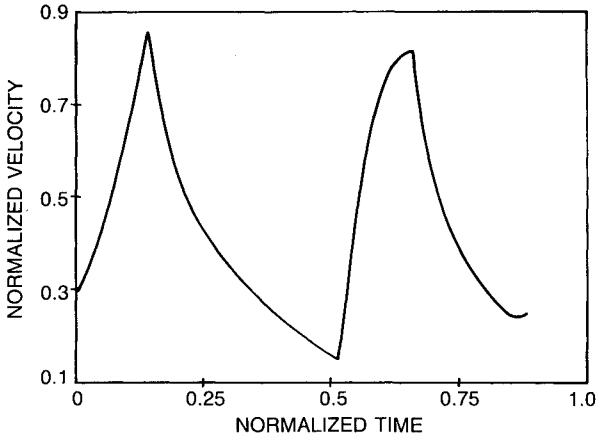

Fig. 4 Altitude constrained trajectory-normalized velocity vs normalized time.

least possible pulse thrust levels and the longest possible pulse burn times. For the 1000-ft (304.8-m) altitude constraint, less is greater than the minimum speed experienced during the interpulse coast period. Note that the coast period exploits virtually all of the potential and kinetic energy without ground impact prior to the second pulse firing. When compared with a candidate trajectory incorporating constant altitude flight, the trajectory and propulsion system optimization resulted in a range improvement of about 30%. Subsequent analysis has established that about 10% of this improvement comes from the propulsion system optimization and around 20% from trajectory optimization.

The optimized trajectory for the high-altitude mission is given in Figs. 7 and 8. The angle of attack history and the pulse motor thrust time curve are in Figs. 9 and 10. For the high-altitude mission, the first pulse called for up to 64% of the total propellant load. The first pulse phase yielded about 7-8 g average acceleration and appeared to strike the best balance between the rate of climb and the aerodynamic losses. The interaction between the required average terminal speed, minimum dynamic pressure, the optimum combination of second pulse thrust, and the interpulse coast time is very complex. However, it appears that the optimal interpulse coast time systematically increased with the decrease in the minimum required dynamic pressure. Interestingly, the optimum ascent trajectories were found to be relatively insensitive to the specified average terminal speed. With a low average terminal speed and a high dynamic pressure at the apogee, the optimization procedure allocated systematically less propellant to the second pulse. At larger values of average terminal speed, the optimum second pulse thrust levels were always less

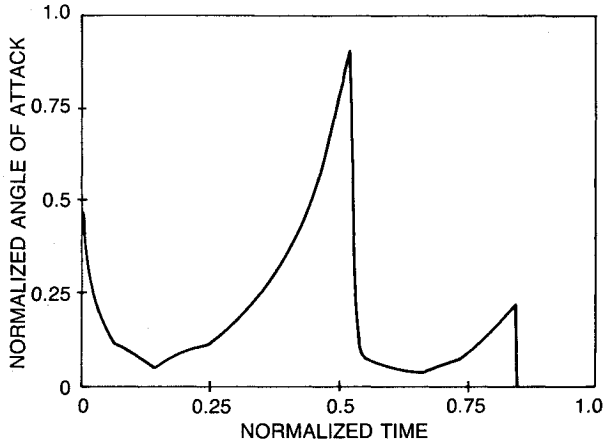

Fig. 5 Altitude constrained trajectory-normalized angle of attack vs normalized time.

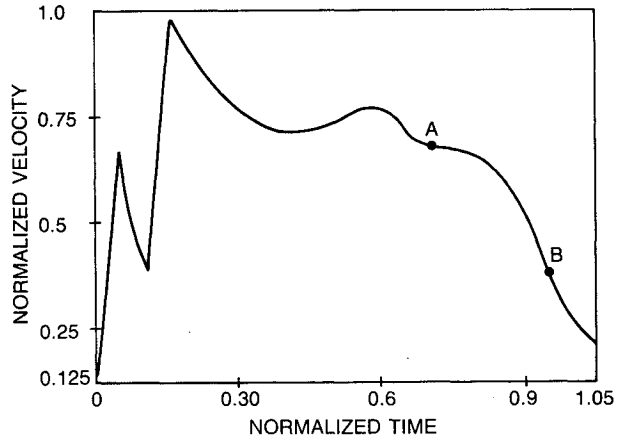

Fig. 8 Minimum dynamic pressure-average terminal speed constrained high-altitude mission: normalized velocity vs normalized time: A) velocity while entering the terminal zone; B) velocity while leaving the terminal zone.

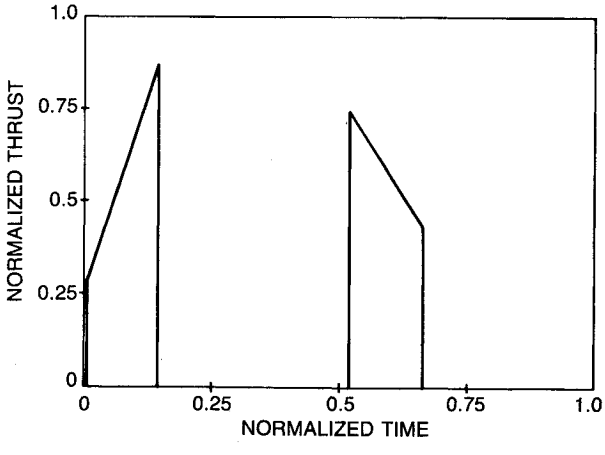

Fig. 6 Altitude constrained trajectory-normalized pulse motor thrust vs normalized time.

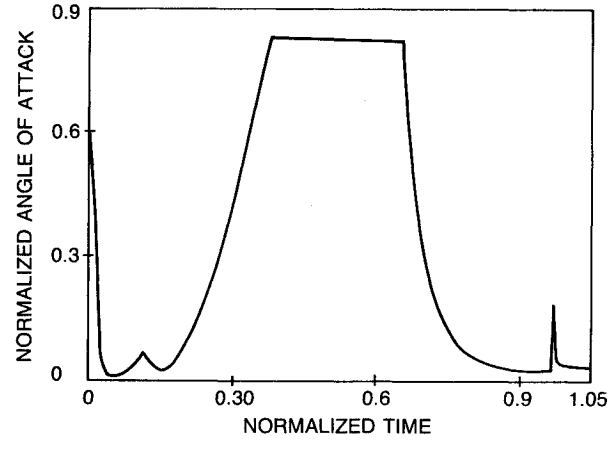

Fig. 9 Minimum dynamic pressure-average terminal speed constrained high-altitude mission: normalized angle of attack vs normalized time.

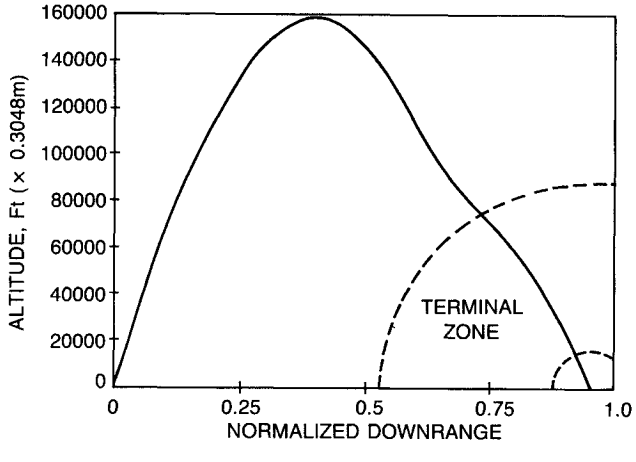

Fig. 7 Minimum dynamic pressure-average terminal speed constrained high-altitude mission: altitude vs normalized range.

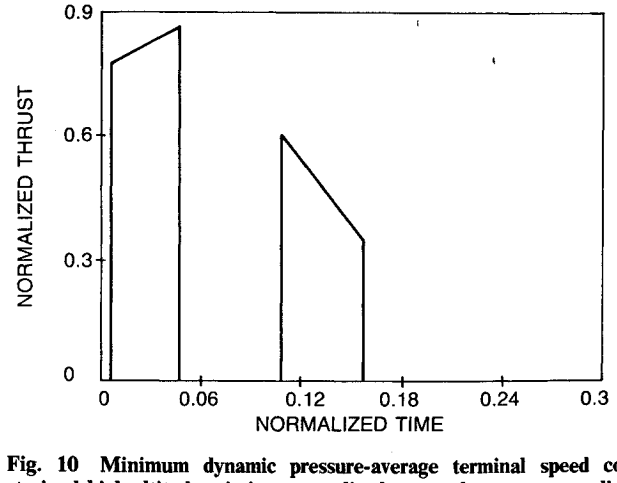

Fig. 10 Minimum dynamic pressure-average terminal speed constrained high-altitude mission: normalized motor thrust vs normalized time.

than those of the first pulse by about 35% regardless of the specific impulse penalty that is imposed for pulse 1/pulse 2 thrust ratio. High-altitude missions with a higher average terminal speed constraint led to as much as 55 deg in the flight path angle in the initial pullup after missile launch. The principal trajectory differences appeared during the descent leg to the target and below 80,000 ft altitude. At low specified average terminal speed, a terminal flare leg is present in the descent trajectory, indicating the conversion of excess energy into downrange.

Conclusions

A nonlinear programming approach for the simultaneous optimization of trajectory and propulsion system for a two-pulse motor propelled air-to-surface missile in two operational scenarios was described. The trajectory control variables, the angle of attack, and the angle of sideslip were parameterized using a combination of piecewise linear open-loop commands and piecewise constant linear feedback gains. The pulse motor parameters optimized were pulse split, neutrality factors (the normalized slope of the thrust-time curves), pulse burn durations and the interpulse delay. A comparison of optimization runs using pure open-loop spline parameterization with the combined open-loop/closed-loop parameterization showed significant reduction in the computing time for the latter while providing nearly the same value for the performance index. In the present study, optimization of the rocket motor in addition to the trajectory increased the downrange by up to 11% when compared with trajectories with completely specified rocket motor propulsion data.

Acknowledgment

This research was supported by AFRPL, Edwards, California, under Contract No. F04611-84-C-0009, via a subcontract from Hercules, Inc.

References

[1]Cheng, V.H.L., Menon, P.K.A., Gupta, N.K., and Briggs, M.M., "A Reduced-Order Approach to Near-Optimal Real-Time Pulse-Motor Ignition Control," AIAA Paper 85-0500, Reno, NV, Jan. 1985; also to appear in the *Journal of Guidance, Control and Dynamics*.

[2]Cheng, V.H.L. and Gupta, N.K., "Advanced Midcourse Guidance of Air-to-Air Missiles," *AIAA Guidance and Control Conference*, Gatlinburg, TN, Aug. 15-17, 1983; also to appear in the *Journal of Guidance, Control and Dynamics*.

[3]Cosentino, G.B. and Holst, T.L., "Numerical Optimization Design of Advanced Transonic Wing Configurations," AIAA Paper 85-0424, Reno, NV, Jan. 1985.

[4]Menon, P.K.A. and Lehman, L.L., "A Parallel Quasi-Linearization Algorithm for Air Vehicle Trajectory Optimization," *Journal of Guidance, Control, and Dynamics*, Vol. 9, Jan-Feb. 1986, pp. 119-121.

[5]Weston, A.R., Cliff, E.M., and Kelley, H.J., "Onboard Near-Optimal Climb-Dash Energy Management," *Journal of Guidance, Control, and Dynamics*, Vol. 8, May-June 1985, pp. 320-324.

[6]Hargraves, C., Johnson, F., Paris, S., and Rettie, I., "Numerical Computation of Optimal Atmospheric Trajectories," *Journal of Guidance and Control*, Vol. 4, July-Aug. 1981, pp. 406-414.

[7]Gilbert, E.G. and Lyons, D.T., "Improved Aircraft Cruise by Periodic Control: the Computation of Optimal Specific Range Trajectories," *Proceeding of the Conference on Information Science and Systems*, Princeton University, March 1980.

[8]Schneider, H. and Reddy, P.B., "Spline Method for Nonlinear Optimal Thrust Vector Controls for Atmospheric Interceptor Guidance," *AIAA Journal*, Vol. 15, April 1977, pp. 449-450.

[9]Johnson, I.L., "Optimization of Solid-Rocket Assisted Space Shuttle Ascent Trajectory," *Journal of Spacecraft and Rockets*, Vol. 12, Dec. 1975, pp. 765-769.

[10]Falco, M. and Kelley, H.J., "Aircraft Symmetric Flight Optimization," *Control and Dynamic Systems*, edited by C.T. Leondes, Vol. 10, 1973, pp. 89-129.

[11]Sheela, B.V. and Ramamoorthy, P., "Optimal Control via Mathematical Programming," *Journal of Guidance and Control*, Vol. 4, July-Aug. 1981, pp. 443-444.

[12]Vinh, N.X., *Optimal Trajectories in Atmospheric Flight*, Elsevier, New York, 1981.

[13]Bryson, A.E. and Ho, Y.C., *Applied Optimal Control*, Blaisdell, Waltham, MA, 1969.

[14]Gill, P.E., Murray, W., and Wright, M.H., Practical Optimization, Academic Press, New York, 1981.

[15]Williamson, W.E., "Use of Polynomial Approximations to Calculate Suboptimal Controls," *AIAA Journal*, Vol. 9, Nov. 1971, p. 2271.

[16]Kelley, H.J. and Denham, W.F., "Examination of Accelerated First-Order Methods for Aircraft Flight Path Optimization," NASA CR-666681, Oct. 1968.